SOLAR DESALINATION UNIT BASED ON HUMIDIFICATION-DEHUMEDIFICATION PROCESSES INTEGRATED WITH FPC

Karima Esmail Amori drkarimaa63@gmail.com
Athraa Hameed Al-Abbasi msc_mechanic@yahoo.com.
University of Baghdad/ College of engineering/ Mechanical Engineering Dept.

ABSTRACT

A humidification-dehumidification (HDH) desalination system integrated with flat plate collector (FPC) was investigated experimentally in an attempt to study the production of fresh water using renewable energy. Two types of solar collectors; concentrated parabolic trough solar collector (to heat oil) and non-concentrated (FPC) (to heat saline water before entering the humidifier) were used in this work. Photovoltaic panels (PV) with DC to AC inverter are used to operate, air fan, oil pump and water pumps. The experiments were carried out in August 2016 under climatological conditions of Baghdad- Iraq (latitude 33.33° N, of longitude 44.4° E). Performance of the HDH system is examined with and without FPC. Saline water was first filtered by a sand filter to reduce water turbidity by (85% – 90%) and is also working to eliminate lichens and the suspended solids from saline water. This filtered saline water was processed through humidification dehumidification system based on solar collector for heat source. Selected water samples are tested for Total Dissolved Salt (TDS) in (mg/l), pH, turbidity in (NTU) and electrical conductivity in (μs/cm) measured before and after desalination process. Before filter the water Turbidity is about (11.2 NTU) while after sand filter it is decreased to (1.94 NTU) and it was (0.1 NTU) after dehumidifier. Results showed that the accumulated productivity is (1050 milliliter); it has been improved by 62%when using FPC.

KeyWords: Desalination, Parabolic Trough Collector (PTC), Humidification-Dehumidification, Fresh water, Flat Plate Collector (FPC).

Received : 2017 -11 - 14
Accepted : 2017 - 11 – 23

List of Symbol

A	Area (m^2)
C_p	Specific heat (J/kg.K)
D	Diameter (m)
F'	Collector efficiency factor
F_R	Collector heat removal factor
F''	Collector flow factor
h	Heat transfer coefficient ($W/m^2.°C$)
I_b	Beam solar radiation (W/m^2)
L	Length (m)
$\dot{m}$	Mass flow rate (kg/s)
Q_u	Useful heat gain of collector (W/m)
Q	Heat transfere (W/m)
Q_{loss}	Loss heat transfer (W)
S	Absorbed solar radiation per unit of aperture area (W/m^2)
T	Temperature (K, °C)
$\bar{T}$	Average temperature between the glass cover and sky (K) temperatures
U	Overall heat transfer coefficient ($W/m^2.°C$)
V	Velocity, speed (m/s)
w	Specific humidity ($kg_{water}/kg_{dry\ air}$)

Greek letters

ε	Emissivity
η	Efficiency
σ	Stefan-Boltzmann constant 5.67×10^{-8} W/m^2K^4

Subscripts

1	Inside of the absorber
2	Outside of the absorber
a	Aperture
abs	Absorber
Amb	Ambient
f	Heat transfer fluid
HDH	Humidification-dehumidification process
i	Inlet
g	Glass
$g,1$	Inside of the glass cover
$g,2$	Outside of glass cover
o	Outlet
$r,abs-g$	Radiation between the absorber and glass cover
$r,g-s$	Radiation between the glass cover and surrounding
sky	Sky
w	Wind

INTRODUCTION

Day after day water scarcity is becoming one of the important and major challenges that the human race on the whole planet faces nowadays, this challenge added to other environment related challenges are becoming problems of global concern that require finding

solutions, reduce the consequences or finding substitutions. One of the substitutions is using desalination to get fresh water from the vast reserves of seawater and saline-water. Solar desalination is a promising technology in the future because solar energy is environmentally friendly **Fath [1998]** and is suitable for a small number of families or small groups in remote areas. Water desalination can be achieved through different technologies such as the Membrane Desalination (MD) and the Humidification (HD) Dehumidification (DHD) processes. Today there are more than 12,506 desalination units in more than 100 countries around the world with a total capacity of 22.8 x 106 m^3/day **Wangnick [1998]**. The success of the desalination industry was a direct result of reducing the cost of unit production. This is achieved by the reduction of the specific equipment size, the development of advanced corrosion-resistant materials, the control of the scale formation, the reduction of specific energy consumption, and ultimately achieve and maintain the plant factor close to 90% **El-Dessouky et al. [1999]**. The HD technique is a thermal process favored for high efficiency and the possibility of integrating them directly with renewable source of energy. The vapor is transferred to the condenser (dehumidifier) utilizing either forced or natural convection where vapor is condenses and acquired as freshwater. The humidification-dehumidification (DHD) desalination process will be investigated in this research. Many researchers have studied different solar desalination configurations. **Bacha et al. [1999]** presented a new generation of water desalination installation by solar energy using the Solar Multiple Condensation Evaporation Cycle (SMCEC) principle. The distilled water obtained by this new concept favors its use for producing water for drinking and irrigation. **Nawayseh et al. [1999]** have conducted a lot of research on the multi-effect humidification dehumidification (MEH) process. This method includes the evaluation of heat and mass transfer coefficients in evaporator, simulation, and so on. The process of solar desalination with the humidification-dehumidification process has proved to be an effective way to use solar energy to produce fresh water from brackish water or sea water. Solar water desalination can be either direct or indirect **Fath [1998]**. The direct solar humidification-dehumidification desalination (HDD) process (solar still) has been investigated by **Nafey et al. [2000, 2001]**. **Nafey et al. [2004]** presented a numerical and experimental investigation of humidification dehumidification desalination process using solar energy at the weather conditions of Suez City, Egypt. The results showed that the productivity of the system is strongly affected by the saline water temperature at the inlet to the evaporator. The condenser cooling water flow rate, air flow rate and solar intensity with wind speed and ambient temperature variation have a very small effect on the system productivity. **Orfi et al. [2004]** studied a solar humidification-dehumidification desalination system to improve the productivity of the system. They utilized the latent heat of condensate water vapor in the condenser to preheat the feed water. **Al-Enezi et al. [2006]** evaluated the characteristics of the humidification dehumidification desalination process as a function of the flow rate of the water and air streams, the temperature of the water stream and the temperature of the cooling water stream. They found the water production is depending strongly on the hot water temperature and it was increased with the increase of the air flow rate and the decrease of the cooling water temperature. **Tiwari et al. [2009]** discussed the effect of water depth on the daily yield of the active solar still integrated with a flat plate solar collector. Results showed that yields decreased with increased water mass. **Feilizadeh et al. [2010]** suggested a new radiation model for single slope solar still to improve its prediction performance. The effect of all walls on the amount of incident solar radiation on the water surface and each wall has been taken into consideration. The experimental data obtained are in good agreement with the theoretical results obtained from the proposed model. **Kabeel et al. [2014]** investigated the effect of three types of forced circulating air (up, down and up-down) on the unit performance is considered. Also, the influence of inlet water temperature and inlet water mass flow rate to the humidifier on the

performance HDH unit was studied. **Yildirim and Solmus [2014]** found that water heated HDH desalination has a significant effect on producing freshwater, due to the higher heat capacity of water as compared to air. Therefore, water heated systems have a significant effect on freshwater produced by systems using flat plate solar collectors for air and water heating. **Hamed et al. [2015]** performed analytical and experimental investigations of solar humidification–dehumidification desalination system. They showed that preheating results in high productivity of about 22 L/day and the total unit cost was about 0.0578 USD/L. **Sandeep et al. [2015]** studied the modified single slope single basin active solar still with improved condensation technique. The researchers found that the modified design showed a productivity increase of 14.5% compared to normal design. The performance of compound parabolic concentrator assisted tubular solar still (CPC-TSS) and compound parabolic concentrator-concentric tubular solar still (CPC-CTSS) (to allow cooling water) with different augmentation systems were studied by **Arunkumar et al. [2016**]. They showed that, the productivity of the un-augmented CPC-TSS and CPC-CTSS were 3710 ml/day and 4960 ml/day, respectively. **Giwa et al. [2016]** investigated the technical feasibility and environmental friendliness of an air-cooled PV system integrated with ambient seawater inflow into a HDH desalination system. They found that the heat recovered from the PV resulted in the production of a daily average of 2.28 lit of freshwater per m^2 of PV. The main objective of this work is to study the thermal performance of solar desalination system based on humidification-dehumidification and investigate the effect of using flat plate collector (FPC) on the performance augmentation of system.Contributions of the present work come from several points, which are not reported in the previous works and can be listed as: Study the thermal performance water evaporator integrated with two types of solar collectors, namely parabolic trough collector (for oil heating) and flat plate collector (for saline water heating).

1. Using a novel design for water evaporator (horizontal basin with horizontal glass cover).
2. Use of U-shaped tube evaporator based on droplet evaporation.

SYSTEM DESCRIPTION

In this work, a humidification–dehumidification (HDH) system integrating with flat plate collector (FPC) has been fabricated and tested at weather conditions in Baghdad, Iraq. The schematic views of the full experimental test rig are shown in Figure (1). Experimentations were carried out on 21st and 22nd August, 2016. The performance of the HDH system was studied with and without FPC. The proposed HDH desalination system consists of rapid sand filter which has four layers of sand and gravel used to remove particles and impurities. Sand filter works to remove 85% to 90% of the turbidity and is also working to eliminate lichens and the suspended solids from saline water. After filtration the saline water flows through two flat plate solar collectors connected in series. Each collector has absorbing area of (1.92 m * 0.85 m) with one glass cover of (4 mm) thickness. the heated saline water is pumped through an electric AC water pump to circulate water in the perforated tube of (13 mm) diameter and (1400 mm) length which drips saline water on the oil heat exchanger (shaped in U-shape tube), both the perforated and the U-shape tubes are located in a horizontal humidification chamber which consists of a galvanized reservoir with a transparent cover, where the dead end perforated tube lies (5 cm) beneath the transparent cover and an oil heat exchanger formed of U-shaped tube placed in the lower part of the reservoir, and its outlet is attached to an oil tank followed by an electric AC gear oil pump to circulate oil. The reservoir was made from galvanized steel of sheet of (6 mm) thickness had the dimensions of (150 cm x 105 cm x 50 cm). The transparent cover was made from glass sheet of (4 mm) thickness and it was vapor-tight. The reservoir was insulated from all five side surfaces by AF/Armaflex class o

sheet insulation of (25 mm) thickness. The reservoir had three holes the first one in the base to drain the redundant water as well as mud and salts deposit. The second hole is on one side of the reservoir; to keep the water level within the required limits by overflowing the excessive water. The third hole is on the same side of the overflow hole and serves as an outlet for the moist air to pass to the dehumidifier. The oil heat exchanger is formed of a copper U-shape tube with a diameter of (19 mm) and a length of (1400 mm). The heated heat transfer fluid (HTF) (oil) is pumped (U-shape tube) in the humidifier where its energy is transferred to the working fluid (water). After transferring its thermal energy to water in the humidifier, the cold HTF leaves the U-shape pipe to an isolated oil tank that feeds the four solar trough collectors in the field. In order to deliver high temperatures with good efficiency a high performance solar collector is required, so four series connected PTCs are used. The reflecting surface of PTC is made of stainless steel plate of (0.5 mm) thickness focusing the sun's energy on an absorber pipe located along its focal line. Each solar receiver consists of riser of a copper tube of (12.25mm) ID, (0.25 mm) thickness and (1700 mm) in length coated with thermal black matt paint, (1500 mm) of its length is used as an absorber and the rest is used for connection. The absorber is covered with glass circular tube to minimize thermal losses and to achieve the greenhouse effect. The length of the glass tube is (1500 mm) and its OD is (25mm) with (0.25 mm) thickness. The collectors are single-axis tracking and aligned on a north-south line, thus tracking the sun from east to west. The PTC supplies hot oil to a U-shaped oil tube while receives cold oil from oil tank. Oil tank is used to supply oil to the solar concentrated trough system. It is insulated from all sides using one layer of thermal insulation of thickness (25 mm) to minimize heat losses; the whole process takes place in a closed loop system. Then the water vapour pass throughout the dehumidifier which consists of a straight channel made from PVC material with (10 cm) diameter, (50 cm) length connected from one end to the humidifier through an aperture to allow the humidified air flow inside the dehumidifier and dehumidify it, the other end of the channel is connected to a fan to extract moist air from the humidifier unit through the channel, also there is a hole in the bottom of the channel to collect the produced condensate water. The channel contains a heat exchanger located at the mid part of it where the dehumidification process takes place on its material surface. The heat exchanger is made of coiled tube of outside and inside diameters are (8 and 7.3) mm respectively with (12) rows and (6) columns in an in-line arrangement. The six columns of the coiled tube are collected in a copper tube distribution header and it is supplied with cooling water by a plastic hose, the heat exchanger takes the cooling water straight from the water channel and returns it back after the heat exchange process to the water channel in an open loop. The whole system uses electric energy in several parts (oil pump, water pumps and a fan) that is supplied from six photovoltaic (PV) panels, hybrid inverter-charge controller, and 4 DC batteries. PV panels are Sharp's ND-220E1J solar module is manufactured by SHARP Company and the type of cell is Polycrystalline silicon. The four batteries are in series connection. Photovoltaic devices generate electricity directly from sunlight. Measuring instruments were installed for recording the experimental data. The data of solar radiation and wind speed were obtained from Ministry of Science and Technology for Baghdad city. Multiple K-type thermocouples with Digital data logger each of 12 channels temperature recorder with SD card data logger model BTM-4208SD manufactured by Lutron company to read and record the magnitude of temperature with an accuracy of (±4%). The temperature measurements range of (-50 to 999.9 ºC) and resolution of (0.1 ºC). Thermocouples are placed and glued with adhesive tape of copper; thermocouples locations distributed in the test rig are given in table (1) and shown in Figure (1). The volumetric flow rate through the dehumidifier was measured by a rotameter of range (5 to 50 l/hr) model LZS-15 Wastewater (PVC flow meter), Yuyao Kingtai Instrument Co., Ltd. The rotameter has an accuracy of (0.04 l/ hr). The average error in flow rate measurement was within (±1.5%) at maximum flow rate of (50 l/

hr). DT266C 3 1/2 DIGITAL CLAMP METER was used to measure voltage and current supplied to the fan and pumps. The voltage resolution is (0.1 V), and its accuracy is (± 0.8%). The current range was from (0.00 to 9.99) A with a resolution of (0.01 A), and accuracy of (± 3.0%). The amount of fresh water productivity was measured using a graduated beaker. The experiments were carried out during a clear sky days for annual test. These tests were adopted to specify the performance of the solar desalination system for different conditions.

The following preparations were made for each test:

1. Cleaning the glass cover of the flat plate solar collectors, the glass cover of the evaporator and the reflected sheets and glass tube of the parabolic trough solar collectors.
2. Connecting all thermocouples to data loggers adjusting date and time recorder of data loggers.
3. The water tank was filled with saline water that was previously filtred via sand filter, the water tanks were frequently checked to ensure the water level.
4. Ensure that all valves are open in the circulation path.
5. Switch on water and oil pumps to circulate the oil and water within the system.
6. All parts of the system were frequently leak checked.
7. Data from all thermocouples were recorded every 10 minutes then checked.

DATA PROCESSING

The generalized thermal analysis of a concentrating collector is convenient to derive appropriate expressions for the collector efficiency factor F', the loss coefficient U_L, and the collector heat removal factor F_R. For a collector of length L the energy loss is calculated as **[Tzivanidis et al, 2015]**:

$$Q_{loss} = \pi D_{g,2} L\left[h_w\left(T_g - T_{amb}\right) + \varepsilon_g \sigma\left(T_g^4 - T_{amb}^4\right)\right] = \pi D_{g,2} L U_L\left(T_g - T_{amb}\right) \quad (1)$$

where L is length of the receiver (m), $D_{g,2}$ is the outside diameter of the glass cover (m), T_g is the temperatures of the glass cover (K), T_{amb} is the ambient temperature (K), ε_g is the emissivity of the glass cover and σ is Stefan-Boltzmann constant (W/m^2.K^4).

In this work the outside and inside temperature of the glass cover is considered the same so the conduction losses are ignored.

The convective heat transfer coefficient from the outer surface of the glass tube to ambient air (h_w) is calculated as **[Mullick & Nanda, 1989]:**

$$h_w = 4V_w^{0.58} D_{g,2}^{-0.42} \quad (2)$$

where V_w wind velocity (m/s).

The useful heat gain of collector Q_u is expressed as [**Duffie & Beckman, 2005**]:

$$Q_u = \frac{A_a}{L} F' \left[S - \frac{A_{abs}}{A_a} U_L\left(T_f - T_{amb}\right)\right] = A_a F_R \left[S - \frac{A_{abs}}{A_a} U_L\left(T_f - T_{amb}\right)\right] \quad (3)$$

where S is the absorbed solar radiation per unit of aperture area (W/m^2), A_a is the apurture area (m^2), A_{abs} is the absorber surface area (m^2), $T_{f,i}$ is the inlet temperature of the working

fluid (oil) (K), and the value of the heat loss coefficient (U_L), is calculated by [**Duffie & Beckman, 2005]:**

$$U_L = \left[\frac{A_{abs}}{A_g\left(h_w + h_{r,g-s}\right)} + \frac{1}{h_{r,abs-g}}\right]^{-1} \quad (4)$$

The radiation coefficient between the glass cover and surrounding ($h_{r,g-s}$) can be calculated from equation suggested by **[Duffie & Beckman, 2005]:**

$$h_{r,g-s} = \varepsilon_g \sigma \bar{T}^3 \quad (5)$$

where $\bar{T}$ is the average temperature between the glass cover and sky temperatures in (K).

The radiation coefficient between the absorber and glass cover ($h_{r,abs-g}$) is calculated as:

$$h_{r,abs-g} = \frac{\sigma\left(T_{abs} + T_g\right)\left(T_{abs}^2 + T_g^2\right)}{\frac{1-\varepsilon_{abs}}{\varepsilon_{abs}} + 1 + \frac{1-\varepsilon_g}{\varepsilon_g}\left(\frac{A_{abs}}{A_g}\right)} \quad (6)$$

where ε_{abs} is the emissivity of the absorber metal, A_g is the surface area of the glass cover (m^2).

The collector efficiency factor *F'* is given as **[Kahrobaian and Malekmohammadi, 2008]**:

$$F' = \frac{1/U_L}{\frac{1}{U_L} + \frac{D_2}{h_f D_1}\left(\frac{D_2}{2k_{abs}}\ln\frac{D_1}{D_2}\right)} = \frac{U_o}{U_L} \quad (7)$$

where D_1 is the inside diameter of the absorber (m) and k_{abs} is the thermal conductivity of the absorber metal (W/m.°C) and (h_f) is the heat transfer coefficient inside tube (W/m^2.°C) and U_o is the overall loss coefficient (W/m^2.°C).

F_R is the heat removal factor is given as **[Norton et. al, 1989]**:

$$F_R = \frac{\dot{m}C_{p_f}}{A_{abs}U_L}\left[1 - exp\left(-\frac{A_{abs}U_L F'}{\dot{m}C_{p_f}}\right)\right] \quad (8)$$

where C_{p_f} is the specific heat of the fluid (J/kg.K).

The collector flow factor F" is then described in following equation:

$$F'' = \frac{F_R}{F'} = \frac{\dot{m}C_{p_f}}{A_{abs}U_L F'}\left[1 - exp\left(-\frac{A_{abs}U_L F'}{\dot{m}C_{p_f}}\right)\right] \quad (9)$$

The solar PTC global thermal efficiency (η_{th}) is defined in the following form:

$$\eta_{th} = \frac{Q_u}{A_a I_b} \quad (10)$$

I_b is beam solar radiation (W/m^2).

The average efficiency (η_{ave}) of the system are calculated as follows **Ghazy A. et al [2016]**:

$$\eta_{ave} = \frac{(M_{HDH})h_{fg}(T)}{\sum_{t=0}^{t=t_{sun}} I\,(T)A_g} \quad (11)$$

where

$$M_{HDH} = \dot{m}_{a,i}\left(\frac{w_i - w_o}{1 + w_i}\right) \quad (12)$$

$$h_{fg}(T) = 2503.3 - 2.398T_{sw} \quad (13)$$

where T_{sw} is saline water temperature (°C), M_{HDH} is the distilled water collected from the dehumidefier that is condensed on heat exchanger (kg/s), h_{fg} is latent heat of evaporation/condensation (J/kg), $\dot{m}_{a,i}$ is mass flow rate of the air (kg/s), w_i and w_o are the air specific humidity at inlet and outlet dehumidefier ($kg_{water}/kg_{dry\ air}$) respectively.

RESULTS AND DISSECTION

The thermal performance of solar desalination system integrated with FPC was analyzed under climatic conditions of Baghdad. On 21st August 2016 the desalination system was first field tested using parabolic trough solar collector only as the basic element that absorbs solar thermal energy to the oil. While the flat plat solar collector was used to preheat the feed water before it enters to the humidifier; this test was carried out on 22nd August 2016. In both test the flow rates of oil, saline water flow rate in perforated tube and cooling water flow rate in the dehumidifier was (72 l/hr), (12 l/hr) and (220 l/hr) respectively. Figure (2) presents the distribution of solar radiation when solar desalination is tested on (21st and 22nd August, 2016). The figure shows that the solar radiation rises from first day hour to reach its maximum value at solar noon, and then ceased to exist at sun set. The maximum solar radiation was (856 W/m^2) at (12:00 pm) on 21st August-16 and decreases after that. Figure (3) shows that the ambient temperature on 21st August it rises from (32.7 ^{o}C) at (9:00 am) to (44.4 ^{o}C) at (13:00 pm). Figure (4 a, b) illustrates the temperature distribution along the absorber surface of the concentrated solar collector. It is found that the surface temperature was increased gradually with length and time. It is reported that the transient absorber surface temperature increases along its length (825 cm) (entrance to exit terminal). This results an increase in oil temperature inside the absorber tube. At 10:00 am the absorber surface temperature was increased from (44.9 ^{o}C) to (66 ^{o}C) along its length, while at 14:00 pm it was increased from (63.9 ^{o}C) to (95.8 ^{o}C) when the system was tested without FPC. While the maximum surface temperature at exit terminal was exceeding (107 ^{o}C) at 14:00 pm when the system was integrated with FPC. The absorber surface temperature was higher than that test without using flat plat solar collector by 9.4% at 12:00 pm. Figure (5) presents the inlet and outlet oil temperature flowing in the absorber from 10:00 am to 14:00 pm. When the system was tested without FPC the oil outlet temperature reached to (95.8 °C) at 14:00 pm while the inlet temperature was (58 °C). The rising in oil temperature was due to the incident solar radiation it was (568.2 W/m^2) at 10:00 am and (716.9 W/m^2) at 14:00 pm. And when the desalination system was integrated with FPC the oil outlet temperature was (106.1 °C) at 14:00 pm while the inlet temperature was (60 °C). The temperatures of the oil flowing in the absorber when the flat plat collector used is obviously higher than that without FPC. The inlet temperature of the oil was increased by 4 % while the outlet oil temperature was increased by 9 %. Figure (6 a, b) presents the temperature history for the surface of U-tube in the evaporator (humidifier). It is clear the surface temperature of U-tube was decreased with its length since hot oil in upper leg of U-tube rejects heat to fallen water droplets, while oil rejects heat from lower leg to surrounding water. Also the U-tube temperature is increased

with time since the solar absorbed energy is increased with time as given in Table (2). when the local time increased from 10:00 am to 14:00 pm the average surface temperature of U-tube increased from (51.8 °C) to (76.4 °C) while it was decreased from (89.9 °C) to (63.1 °C) along its length at 14:00 pm (entrance terminal to exit terminal). The temperature values of the desalination system with FPC are higher than that test without using FPC. when the desalination system was integrated with FPC The average surface temperature of U-tube increased from (53.3 °C) to (81.1 °C) when the local time increased from 10:00 am to 14:00 pm while it was decreased from (97.4 °C) to (71.4 °C) along its length at 14:00 pm (entrance terminal to exit terminal). The enhancement of the average surface temperature of U-tube when the PTC was used is shown in Table (3). The saline water energy content is calculated as:

$$Q = \dot{m}_w C_{p,w} \Delta T \qquad (14)$$

where Q is the saline water energy content (W), $\dot{m}_w$ is the saline water mass flow rate (kg/s), $C_{p,w}$ is the specific heat of saline water (J / kg °C) and ΔT is the temperatures difference between two hours (°C). Figure (7) shows the energy distribution along the perforated tube. The energy distribution along the perforated tube was approximately constant along the period of hour. when the desalination system was tested without using FPC this energy was increased from (30.2 W) to (139.5 W) with increased time from (10:00 am) to (14:00 pm), while when the system was tested with FPC this energy was increased from 10:00 am to 12:00 pm then it was decreased from 13:00 pm and14:00 pm due to decreased of incident solar radiation. Table (4) shows the saline water energy content entered to perforated tube for the two cases with and without FPC it was clear there is an enhancement of energy content when the FPC was used. The continuous line represents the test with the FPC while the dotted line represents the test without FPC. Figure (8) illustrates the inlet and outlet temperatures of the cooling water in dehumidifier. The time affects the cooling water temperature which it is increased with time. The inlet cooling water temperature was not affected by FPC while the outlet cooling water temperature was increased by an average percent of 10% when it is compared to tests without FPC. This increment in temperature of the dehumidifier chamber is due to the rise in temperature of wet air inside the humidification chamber which is passing through the heat exchanger in the dehumidifier chamber. The difference between the outlet and inlet cooling water temperature was (5 ºC) at 12:00 pm when test was without using FPC while this difference was increased to (9 ºC) when the FPC was used. Figure (9) shows the productivity of distilled water for a test extended from 9:00 am to 14:00 pm. It is reported that (105 ml) was obtained at 10:00 am and accumulated to reach (1050 ml) at 14:00 pm when the system was tested without FPC while the productivity was increased from (230 ml) at 10:00 am to (1505 ml) at 14:00 pm when the desalination system was tested with FPC. Higher water production is reported (as 62%) when FPC is used to heat the saline water. This increase is due to use two sources of collecting solar energy (concentrated (PTC) and non-concentrated (FPC) solar collector) which was caused to increase the system temperature that leads to increase the rate of saline water evaporation and therefore increased the productivity of the distilled water. Figure (10) illustrates the useful energy gain for the PTC increased to its maximum value (709.07W) at (13:00 pm) when FPC was not used while it was (674.28W) when FPC was used. This is due to the inversely proportional between useful energy and oil inlet temperature which it was increased when FPC was used. Figure (11) presents the relation between the variation of solar radiation and the thermal efficiency of PTC. It is noted that increasing of the solar radiation causes a decrease in the thermal efficiency. Maximum efficiency at (10:00 am) was (0.76) when FPC was not used while it was decreased to (0.73) when FPC was used. This decrease is due to inversely proportional between inlet fluid

temperature to the PTC and efficiency; in which the fluid inlet temperature was increased when the FPC was integrated with the desalination system. Figure (12) illustrates the variation of heat loss coefficient along the absorber with time. It can be noticed that it is increased with the time. The heat loss coefficient was generally dependent on the heat transfer coefficients and it is determined by measured value of ambient, glass cover and absorber surface temperatures. The heat loss coefficient at (14:00 am) was (8.57 W/m^2.K) when FPC was used while it was decreased to (7.98 W/m^2.K) when FPC was not used this decreases due to decrease temperatures of the glass cover and absorbers. Figure (13) reports the variation of the heat removable factor with time. It is found that the heat removal factor decreases with time. When FPC was not used the heat removable factor at (10:00 am) was (0.92) while it was decreased to (0.89) when FPC was used, this decrease due to the increase of heat loss coefficient when FPC was integrated with the system.

RESULTS OF TESTED WATER QUALITY

The water quality analysis was performed at Ministry of Science and Technology Department of Environment and Water Technology. The results obtained are presented in Table (5) for selected water samples (A, B, C and D). These samples are tested for their Total Dissolved Salt (TDS) in (mg/l), pH, turbidity in (NTU) and electrical conductivity in (µs/cm) measured before and after desalination. Before desalination the conductivity in the water was about (669.7 µs/cm) which is not drinkable. However, after desalination it decreased to (0.08 µs/cm) which is drinkable. The typical pH varies from one water sample to another as well as on the nature of the construction materials used in the water distribution system. It is usually in the range of 6.5–8. Before filter the water Turbidity is about (11.2 NTU) while after filter it decreased to (1.94 NTU).

ERROR ANALYSIS

The accuracy of obtained experimental results depends upon two factors: the accuracy of measurements and the nature of rig design. There is no doubt that, the maximum portion of errors in calculations referred essentially to the errors in the measured quantities.

Thermal efficiency (η) is a function of different variables namely (temperature, solar radiation, mass flow rate). Table (6) shows the accuracy of parameters used in the calculation of the error analysis. Hence, to calculate the error in the obtained results, presented in **Holman, (1989)** the percentage error of the collector efficiency is calculated as:

$$w_R = \left[\left(\frac{\partial R}{\partial x_1} w_1\right)^2 + \left(\frac{\partial R}{\partial x_2} w_2\right)^2 + \cdots + \left(\frac{\partial R}{\partial x_n} w_n\right)^2\right]^{1/2} \quad (15)$$

$$w_\eta = \left[\left(\frac{\partial \eta}{\partial \Delta T} w_{\Delta T}\right)^2 + \left(\frac{\partial \eta}{\partial I_T} w_{I_T}\right)^2 + + \left(\frac{\partial \eta}{\partial \dot{m}} w_{\dot{m}}\right)^2\right]^{1/2} \quad (16)$$

where w_R is the uncertainty in the result and $w_1, w_2 \ldots w_n$ is the uncertainty in the independent variables.

Example:

$$\dot{m} = 0.0175\frac{kg}{s}, \qquad I_T = 743\frac{W}{m^2}, \qquad A_a = 0.9\ m^2, \qquad C_p = 1964\frac{J}{kg.K}$$

$$\frac{\partial \eta}{\partial \Delta T} = \frac{\dot{m}C_p}{I_T A_a} = \frac{0.0175 \times 1964}{743 \times 27} = 1.7 \times 10^{-3}$$

$$\frac{\partial \eta}{\partial I_T} = -\frac{\dot{m}C_p \Delta T}{{I_T}^2 A_a} = -\frac{0.0175 \times 1964 \times 27}{743^2 \times 0.9} = -1.87 \times 10^{-3}$$

$$\frac{\partial \eta}{\partial \dot{m}} = \frac{C_p \Delta T}{I_T A_a} = \frac{1964 \times 27}{743 \times 0.9} = 79.3$$

$$w_\eta = [(1.7 \times 10^{-3} \times 0.1)^2 + (-1.87 \times 10^{-3} \times 10)^2 + (79.3 \times 0.0004)^2]^{1/2}$$

$$w_\eta = 0.036$$

CONCLUSIONS

The desalination system was tested using parabolic trough solar collector only as energy source (with and without flat plate collector) then with flat plate solar collector, the conclusions extracted are:

1. Integrating the system with FPC causes an increase in saline water temperature in perforated tube by 11% at 12:00 am.
2. Oil temperature in U-shaped tube is increased by 11.8 % at 12:00 pm when using FPC.
3. The fresh water productivity is increased by 62% due to integrating the system with FPC.

Tabe (1): Thermocouples Locations

Thermocouples NO.	Place
1, 2,..., 6	Evaporater (for saline water in perforated tube)
7	Evaporater (for vapor)
8 & 9	Condenser (inlet and outlet cooling water)
10, 11,… 21	Absorber surface tube
22, 23,… 31	U-shaped tube
32,33,…, 35	Glass cover of evaporater
36 &37	Condenser (inlet and outlet moisture air)
38	Ambient
39 & 40	Wet bulb temperature
41 & 42	Inlet and outlet to FPC
43	Saline water inlet to evapotator
44	Saline water in the base of evaporator

Table (2) U-Tube Temperature Distribution without FPC

Time (hr)	T_A (°C)	T_B (°C)	T_C (°C)	T_D (°C)	$\frac{T_A-T_B}{T_A}$(%)	$\frac{T_C-T_D}{T_C}$(%)
10:00 am	58.9	54	51.9	43.1	8.3	17.0
12:00 pm	72.1	63.1	62	56.2	12.5	9.3
14:00 pm	89.9	79.4	75.3	63.1	11.7	16.2

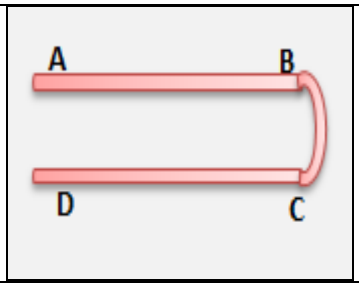

Table (3) Enhancement of the Average Surface Temperature of U-Tube with PTC

Time (hr)	Without FPC Temperature (°C)	With FPC Temperature (°C)	Percentage Enhancement %
10:00 am	51.8	55.3	6.3
11:00 am	57.2	61.7	7.3
12:00 pm	63.8	71.7	11.0
13:00 pm	72.1	75.8	4.9
14:00 pm	76.4	80.9	5.6

Table (4) Energy Content of Saline Water Entered to Perforated Tube

Time (hr)	Energy without FPC (W)	Energy with FPC (W)	Percentage Enhancement %
10:00 am	16.27	299.85	17.43
11:00 am	51.14	436.99	7.55
12:00 pm	99.95	581.11	4.81
13:00 pm	118.55	453.26	2.82
14:00 pm	125.52	416.08	2.31

Table (5) Tested Water Quality Results

Sample	TDS(mg/l)			PH			Turbidity (NTU)			Conductivity (µs/cm)		
	Before filter	Before desalination (After filter)	After desalination	Before filter	Before desalination	After desalination	Before filter	Before desalination	After desalination	Before filter	Before desalination	After desalination
A	324	324	0.08	7.38	7.38	7.25	10.8	1.23	0.03	585	585	0.1
B	356	356	0.05	7.9	7.9	6.7	10.3	1.53	0.05	630.6	630.6	0.09
C	292	292	0.05	7.8	7.8	7.1	10.5	1.1	0.09	529.3	529.3	0.05
D	371	371	0	7.4	7.4	6.3	11.2	1.94	0.1	669.7	669.7	0.08

Table (6): Accuracy of parameters used in the calculation of the error analysis

Independent Variables	Mass flow rate	Solar Radiation	Temperature
Uncertainty interval	0.0004	±10 W/m^2	±0.1 ºC

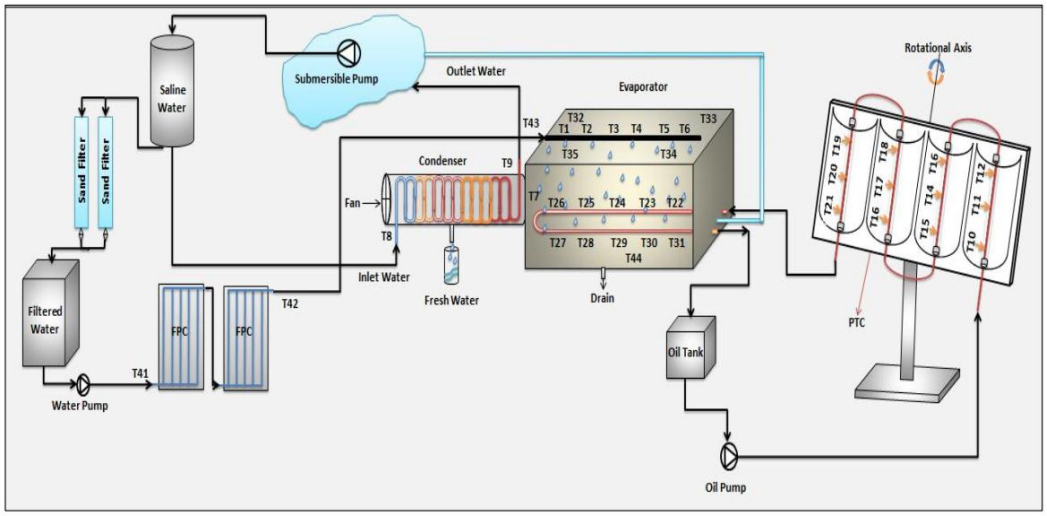

Fig.(1) Schematic diagram for outdoor experimental setup with thermocouple locations

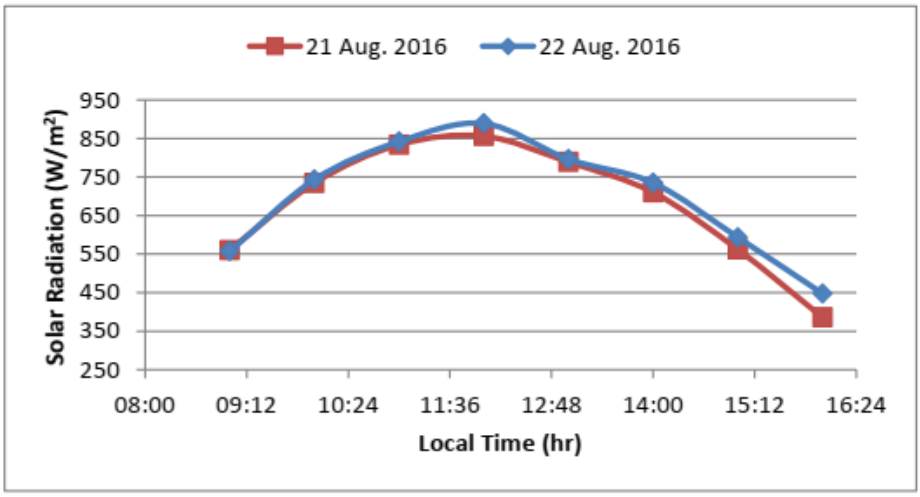

Fig. (2) Variation of Solar Radiation with Local Time

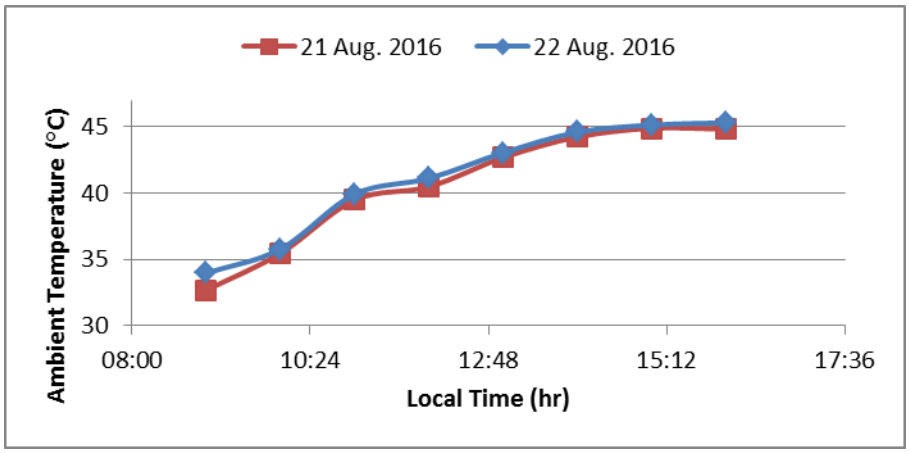

Fig. (3) Variation of Ambient Temperature with Local Time

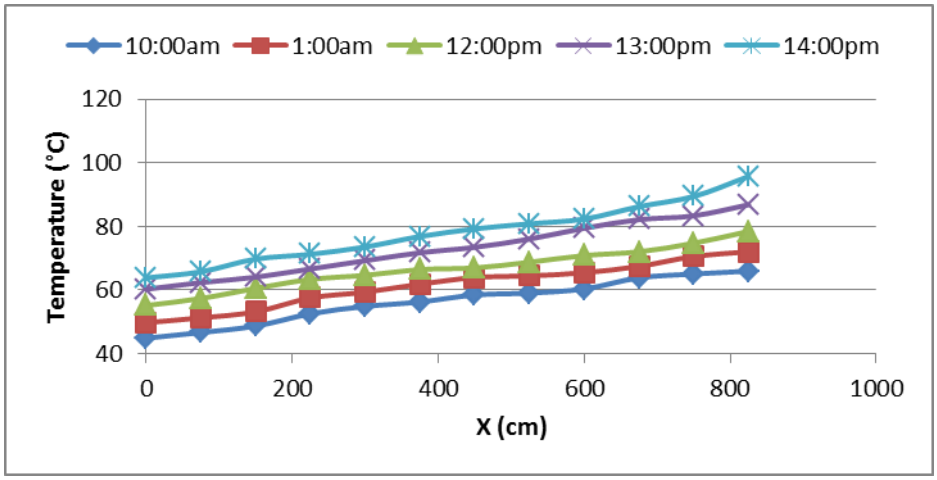

(a)Without FPC

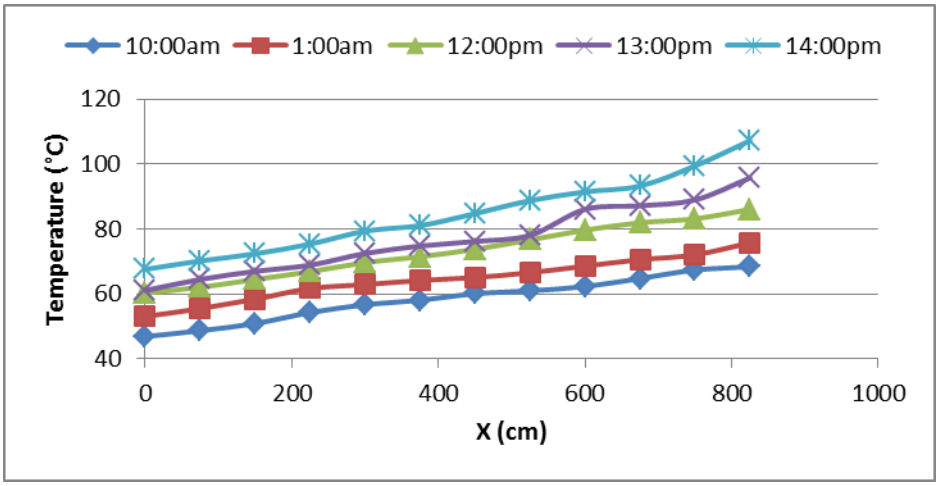

(b)With FPC

Fig. (4 a, b): History of Absorber Surface Temperature

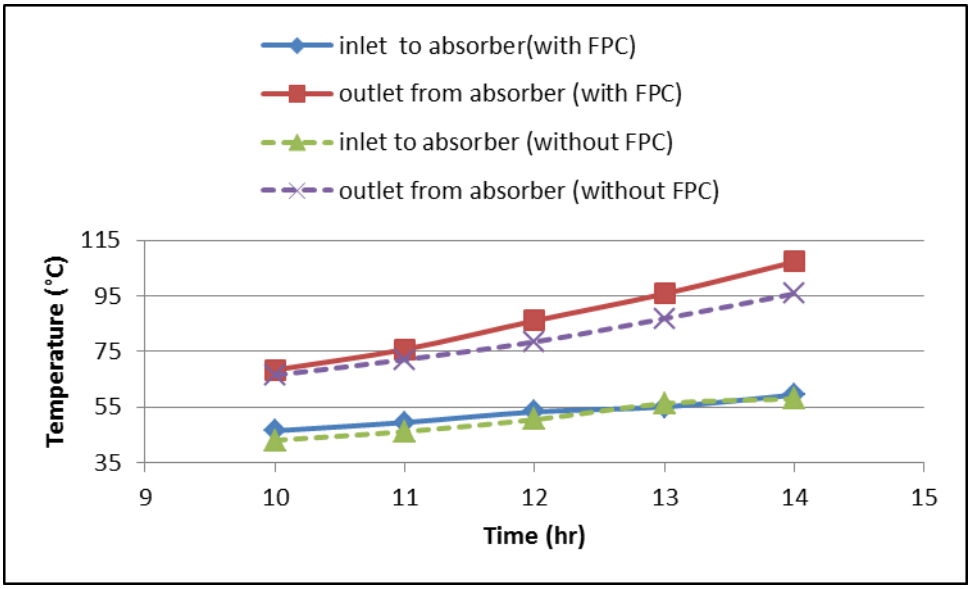

Fig. (5): History of Oil Inlet and Outlet Temperature with and without FPC

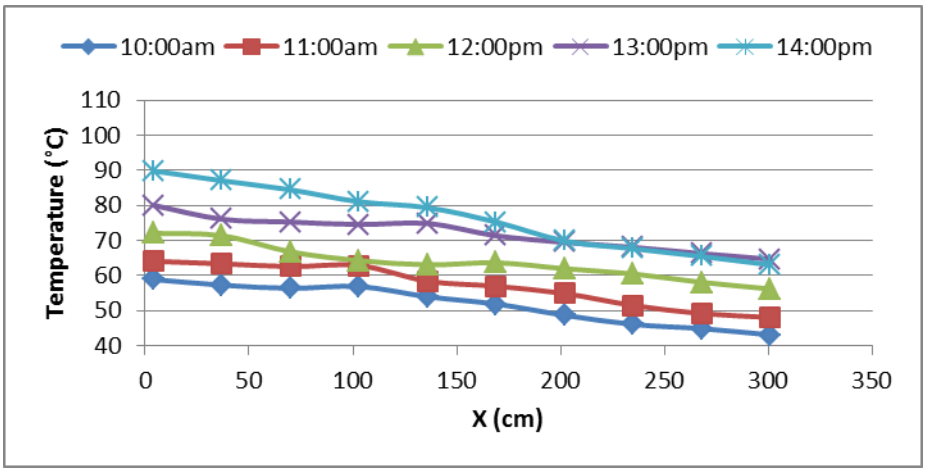

(a)Without FPC

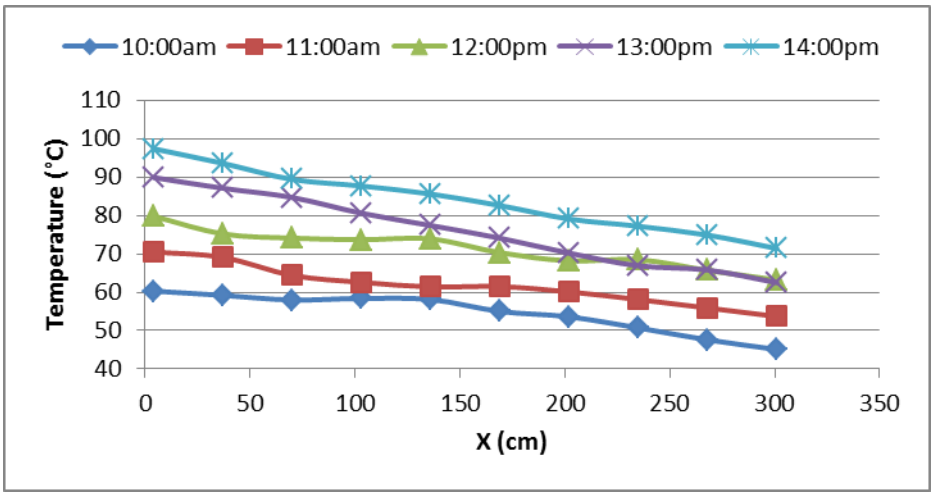

(b)With FPC

Fig. (6 a, b): History of Temperature along the U-Tube

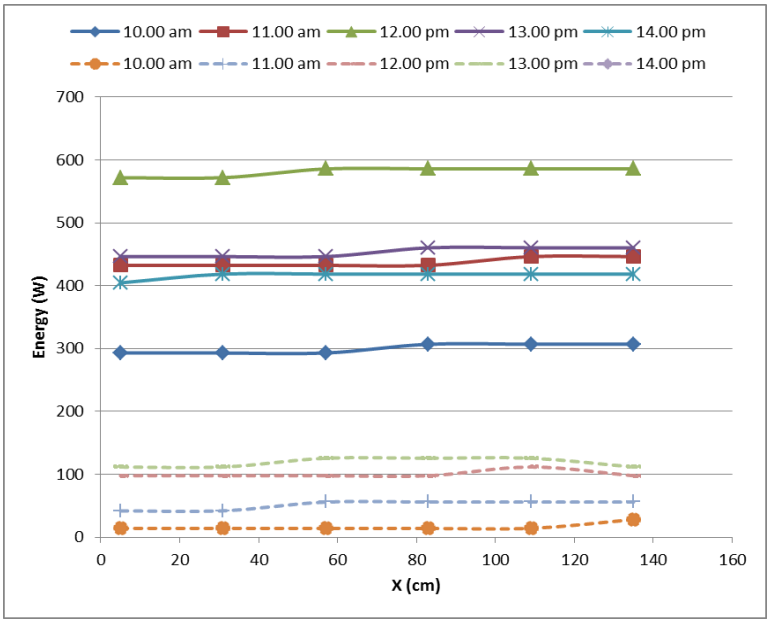

Fig. (7): Effect of Integrating the Desalination Unit with FPC on Saline Water Energy Content in Perforated Tube

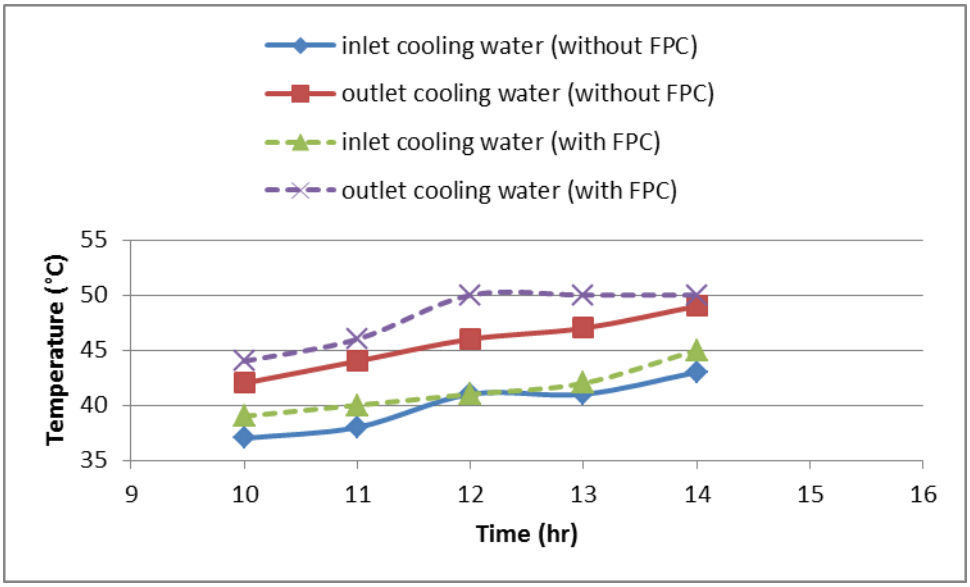

Fig. (8): History of Inlet and Outlet Cooling Water Temperature in Dehumidifier with and without FPC

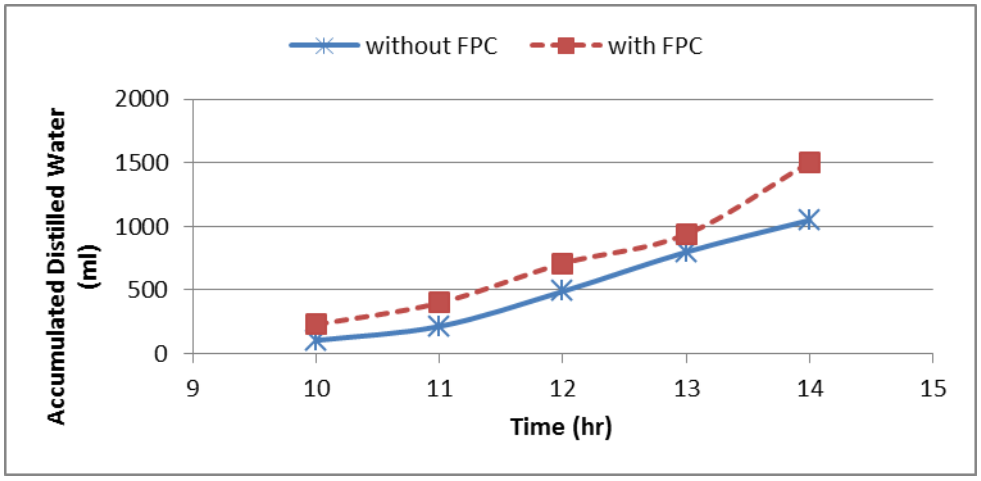

Fig. (9): Accumulative Fresh Water Productivity with and without FPC

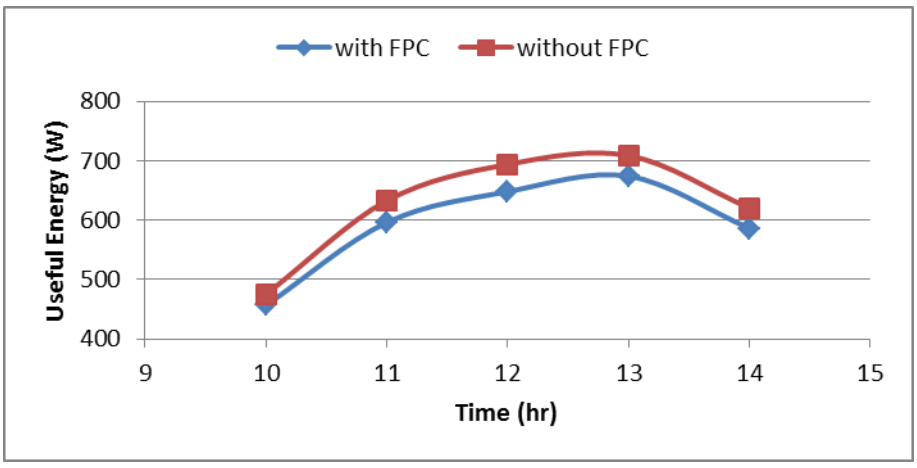

Fig. (10) Variation of Useful Energy of PTC with Local Time

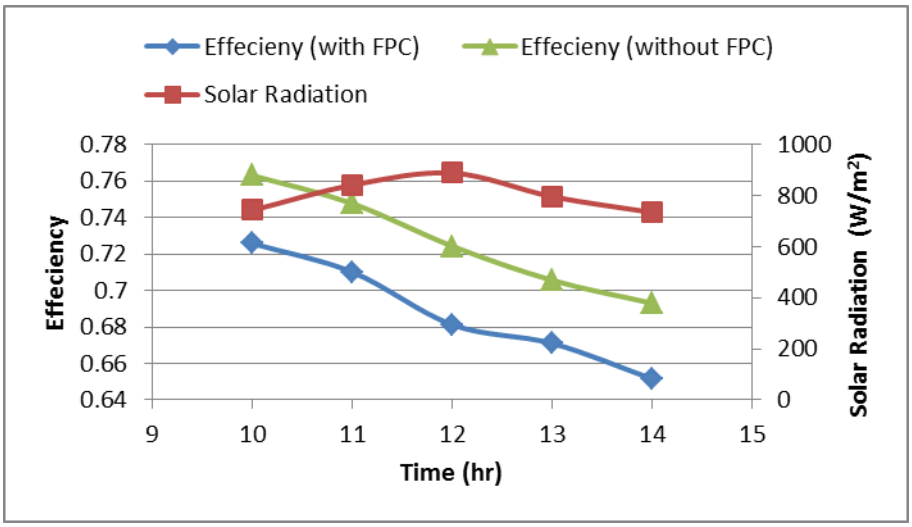

Fig. (11) Variation of Solar Radiation and Thermal Efficiency of PTC with Local Time

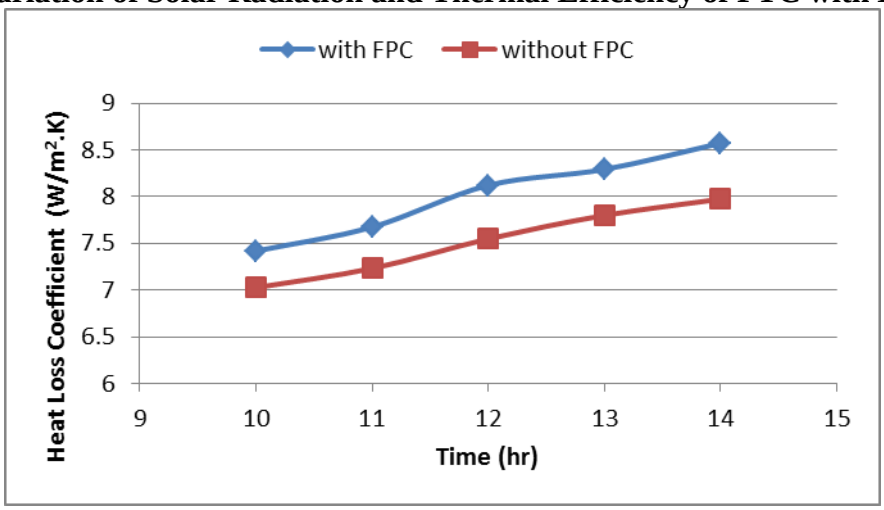

Fig. (12): Variation of Heat Loss Coefficient along the Absorber with Local Time

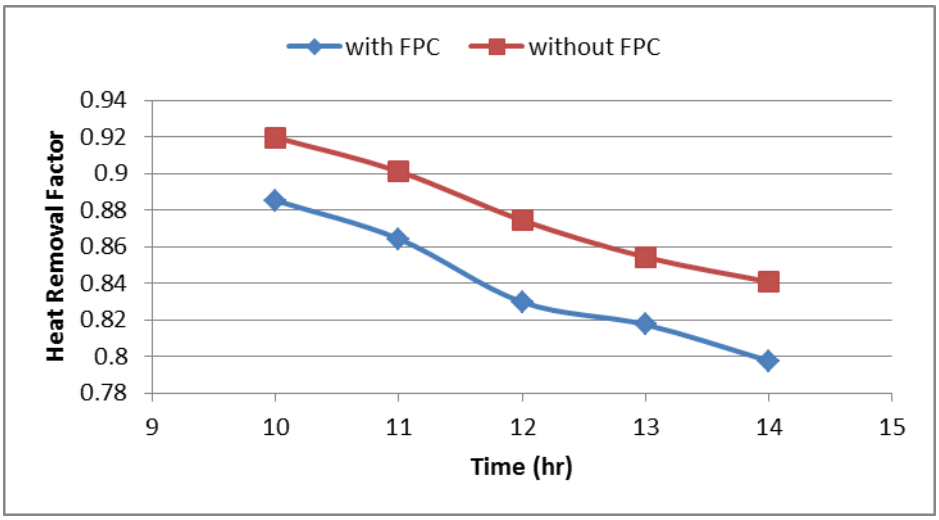

Fig. (13) Variation of Heat Removal Factor with Local Time

Acknowledgment

This research was supported and funded by University of Baghdad, College of Engineering, Department of Mechanical Engineering and UNICEF.

REFERENCES

Al-Enezi G., Ettouney H., Fawzy N., (2006), "Low temperature humidification dehumidification desalination process", Energy Conversion and Management, V47, pp.470–484.

Arunkumar T., Jayaprakash R., Ahsan A., Denkenberger D., Okundamiya M.S., (2013), " Effect of water and air flow on concentric tubular solar water desalting system", Applied Energy, V.103, pp.109–115.

Arunkumar T., Velraj R., Denkenberger D.C., Ravishankar Sathyamurthy, Kumar K. V., Ahsan A., (2016), " Productivity enhancements of compound parabolic concentrator tubular solar stills", Renewable Energy, V88, pp. 391-400.

Bacha B. H., Bouzguenda M., Abid M.S., Maalej A.Y., (1999), "Modeling and simulation of a water desalination station with solar multiple condensation evaporation cycle technique", Renewable Energy 18, pp.349-365.

Duffie J.A., Beckman W. A., (2005), "Solar Engineering of Thermal Process", Wiley Interscience Publications, John Wiley & Sons, New York.

El-Dessouky H.T., Ettouney H.M., Al-Al-Juwayhel F., (1999), "Four decades for the multi-stage Flash desalination" in: Fourth Gulf Water Conference, Bahrain.

Fath H., (1998), "Solar desalination promising alternative for fresh water production with free energy, simple technology and clean environmental", Desalination, V 116, pp. 45–56.

Feilizadeh M., Soltanieh K., Jafarpur M.R., Karimi Estahbanati, (2010), "A new radiation model for a single-slope solar still", Desalination, V262, pp. 166-173.

Ghazy A., Hassan E. S. Fath H., (2016), "Solar desalination system of combined solar still and humidification–dehumidification unit", Heat Mass Transfer, pp. 1761-1.

Giwa A., Fath H., Hasan S. W., (2016), "Humidification-dehumidification desalination process driven by photovoltaic thermal energy recovery (PV-HDH) for small-scale sustainable water and power production", Desalination, V377, pp.163–171.

Hamed M.H., Kabeel A.E., Omara Z.M., Sharshir S.W., (2015), "Mathematical and experimental investigation of a solar humidification–dehumidification desalination unit", Desalination, V 358, pp. 9–17.

Holman, E. W., (1989), "Some evolutionary correlates of higher taxa", Paleobiology, V 15, pp. 357-363.

Kabeel A.E., Mofreh H.H., Omara Z.M., Sharshir S.W., (2014), "Experimental study of a humidification-dehumidification solar technique by natural and forced air circulation", Energy, V68, pp.218-228.

Kahrobaian A. and Malekmohammadi H., (2008), "Exergy Optimization Applied to Linear Parabolic Solar Collectors", Journal of Faculty of Engineering, V42, No. 1, pp. 131-144.

Mullick S.C., Nanda S.K., (1989), "An Improved Technique for Computing the Heat Loss Factor of a Tubular Absorber"; Solar Energy; V42; Issue 1, pp. 1-7.

Nafey A. S., Abdelkder M., Abdelmotalip A., Mabrouk A. A., (2001) "Enhancement of solar still productivity using floating perforated black plate", Energy Convers Mgmt, V 43, pp.1401–1408.

Nafey A. S., Fath H., El-Helaby S. O., Soliman A. M., (2004) "Solar desalination using humidification dehumidification processes, Part I a numerical investigation", Energy Convers Manag, V 45, pp. 1243-1261.

Nafey A. S., Fath H., El-Helaby S. O., Soliman A. M., (2004) "Solar desalination using humidification dehumidification processes, part II an experimental investigation. Energy Convers Manag, V 45, pp. 1263-1277.

Nafey AS, Abdelkder M, Abdelmotalip A, Mabrouk A. A., (2000) "Parameters affecting solar still productivity". Energy Convers Mgmt, V 41, pp.1797–1809.

Nawayseh N.K., Farid M.M., Al-Hallaj S., Al-Timimi A.R., (1999), "Solar desalination based on humidification process: I—evaluating the heat and mass transfer coefficients", Energy Convers. Manag. V40, No.13, pp. 1423–1439.

Nawayseh N.K., Farid M.M., Omar A.A., Sabirin A., (1999), "Solar desalination based on humidification process: II—computer simulation", Energy Convers. Manag. V40, No. 13, pp. 1441–1461.

Norton B., Prapas D. E., Eames P. C., Propert S. D., (1989), "Measured Performances of Curved Inverted-Vee, Absorbed Compound Parabolic Concentrating Solar-Energy Collectors", Solar Energy, V43, No. 5, pp. 267-279.

Orfi J., Laplante M., Marmouch H., Galanis N., Benhamou B., Nasrallah S. B., Nguyen C.T., (2004) "Experimental and theoretical study of a humidification–dehumidification water desalination system using solar energy", Desalination No. 168, pp151–159.

Sandeep, Sudhir Kumar, Dwivedi V.K., (2015), "Experimental study on modified single slope single basin active solar still", Desalination, V 367, pp. 69-75.

Tiwari G.N., Dimri V., Chel A., (2009), "Parametric study of an active and passive solar distillation system: energy and exergy analysis", Desalination, V 242 pp. 1–18.

Tzivanidis C., Bellos E., Korres D., Antonopoulos K.A., Mitsopoulos G., (2015), " Thermal and optical efficiency investigation of a parabolic trough collector", Case Studies in Thermal Engineering, V 6, pp. 226–237.

Wangnick K., (1998), New IDA worldwide desalting plants inventory, Int. Desalination and Water Reuse 8, pp. 11-12.

Yildirim C, Solmus I., (2014), "A parametric study on a humidification-dehumidification (HDH) desalination unit powered by solar air and water heaters", Enersgy Convers Manage, V 86, pp. 568–575.